The Journal of Neuroscience, May 1, 2001, 21(9):3092–3103

The Expression Pattern of the Cell Cycle Inhibitor p19^{INK4d} by Progenitor Cells of the Rat Embryonic Telencephalon and Neonatal Anterior Subventricular Zone

Volkan Coskun and Marla B. Luskin

Department of Cell Biology, Emory University School of Medicine, Atlanta, Georgia 30322

In this study we investigated whether the pattern of expression of the cyclin-dependent kinase inhibitor p19^{INK4d} by the unique progenitor cells of the neonatal anterior subventricular zone (SVZa) can account for their ability to divide even though they express phenotypic characteristics of differentiated neurons. p19^{INK4d} was chosen for analysis because it usually acts to block permanently the cell cycle at the G_1 phase. p19^{INK4d} immunoreactivity and the incorporation of bromodeoxyuridine (BrdU) by SVZa cells were compared with that of the more typical progenitor cells of the prenatal telencephalic ventricular zone. In the developing telencephalon, p19^{INK4d} is expressed by postmitotic cells and has a characteristic perinuclear distribution depending on the laminar position and state of differentiation of a cell. Moreover, the laminar-specific staining of the developing cerebral cortex revealed that the ventricular zone (VZ) is divided into p19^{INK4d}(+) and p19^{INK4d}(−) sublaminae, indicating that the VZ has a previously unrecognized level of functional organization. Furthermore, the rostral migratory stream, traversed by the SVZa-derived cells, exhibits an anterior^{high}–posterior^{low} gradient of p19^{INK4d} expression. On the basis of the p19^{INK4d} immunoreactivity and BrdU incorporation, SVZa-derived cells appear to exit and reenter the cell cycle successively. Thus, in contrast to telencephalic VZ cells, SVZa cells continue to undergo multiple rounds of division and differentiation before becoming postmitotic.

Key words: cyclin-dependent kinase inhibitors; p19^{INK4d}; progenitor cells; proliferation; subventricular zone; ventricular zone

During development the proliferating cells within the ventricular and subventricular zones that line the lateral ventricles give rise to the neurons of the mammalian forebrain. From tritiated thymidine and bromodeoxyuridine (BrdU) birth-dating studies and the staining patterns of cell type-specific markers (Brand and Rakic, 1979; Menezes and Luskin, 1994; Kornack and Rakic, 1998) current thinking suggests that the progenitor cells of the telencephalic ventricular zone (VZ) give rise to cells that exit the mitotic cycle at the ventricular surface and then undergo differentiation and migration (Rakic, 1974; Bayer et al., 1991). The specialized neuronal progenitor cells located within the anterior part of the subventricular zone of the postnatal forebrain (SVZa) (Luskin, 1993) constitute the major exception to this orderly process, by which proliferation precedes differentiation and migration (Menezes et al., 1995). In particular, as the progeny of the SVZa cells migrate to the olfactory bulb along a restricted pathway, the rostral migratory stream (RMS), they concurrently undergo division, despite expressing a neuronal phenotype. Thus, unlike the cells of the VZ, SVZa-derived cells initiate differentiation before becoming postmitotic.

An obligatory step for a cell to become postmitotic is considered to be the withdrawal from the cell cycle at the G_1 phase, before reentry into the S phase (Sherr, 1994). Progression from G_1 to S phase is negatively regulated by two families of cyclin-dependent kinase inhibitors (CDKIs), the CIP/KIP and INK4 families (Hirai et al., 1995; Weinberg, 1995; Sherr and Roberts, 1999). An analysis of the INK4 family consisting of p15^{INK4b}, p16^{INK4a}, p18^{INK4c}, and p19^{INK4d} has revealed that they exhibit differential expression patterns. In particular, p18^{INK4c} and p19^{INK4d} are expressed during neurogenesis, whereas p15^{INK4b} and p16^{INK4a} are absent during development (Zindy et al., 1997a,b). Moreover, p27^{KIP1}, a member of the CIP/KIP family, was shown to be essential for cell cycle exit mechanisms as well as the differentiation of oligodendrocytes (Raff et al., 1998; Tikoo et al., 1998; Casaccia-Bonnefil et al., 1999). The involvement of CIP/KIP proteins in the genesis of neurons has not been elucidated. The INK4 family members, specifically p18^{INK4c} and p19^{INK4d}, however, have been suggested to play a role in the development of both the cerebral cortex (Zindy et al., 1997b, 1999) and cerebellum (Watanabe et al., 1998). Thus, INK4 proteins might couple proliferation arrest to terminal differentiation by cell cycle arrest at G_1.

An understanding of how proliferation is inversely coupled to differentiation during cortical development must take into account the cellular kinetics that progenitor cells undergo. As the VZ cells proliferate, their nuclei oscillate in a process referred to as "interkinetic nuclear migration," such that there is a relationship between the position of the nucleus and the phase of the cell cycle (Takahashi et al., 1996). During G_1, the nuclei ascend from the ventricular surface to the basal border of the VZ, whereas in S phase they undergo DNA synthesis (see Fig. 1). In G_2, nuclei return to the ventricular surface before entering the M (mitotic) phase. An individual progenitor cell can divide either symmetrically (both daughter cells either become postmitotic or prolifer-

Received Aug. 29, 2000; revised Feb. 2, 2001; accepted Feb. 8, 2001.

This work was supported by the National Institute on Deafness and Other Communication Disorders Grant RO1 DC03190 to M.B.L. We thank Christopher P. Noyes for his technical assistance and the members of the lab of M.B.L. for their helpful comments on this manuscript. We are also grateful to Drs. Douglas Falls and Kevin Moses for their suggestions and valuable comments on this manuscript.

Correspondence should be addressed to Dr. Marla B. Luskin, Department of Cell Biology, Emory University School of Medicine, 1648 Pierce Drive, Atlanta, GA 30322. E-mail: luskin@cellbio.emory.edu.

ate) or asymmetrically (one daughter cell becomes postmitotic and the other continues to proliferate).

In this study, we have investigated whether the unusual proliferative capacity of SVZa progenitor cells can be explained by a differential regulation of the G_1–S progression. Therefore, we have compared the p19^{INK4d} expression pattern of the cells of the postnatal SVZa and RMS with that of telencephalic VZ cells. We demonstrated an anterior^{high}–posterior^{low} gradient of p19^{INK4d} expression along the RMS, indicating that few cells withdraw from the cell cycle in the SVZa and increasingly more as the olfactory bulb is approached. In addition, we showed that the VZ is comprised of a predominantly p19^{INK4d}(+) sublamina (apposed to the ventricular surface) and a predominantly p19^{INK4d}(−) sublamina, indicating that VZ can be divided on the basis of its pattern of p19^{INK4d} expression. Furthermore, the intracellular localization of p19^{INK4d} varies as a function of the laminar position of a cell in the developing cerebral cortex, suggesting that p19^{INK4d} is dynamically regulated.

MATERIALS AND METHODS

BrdU injections and perfusion. To obtain embryos of particular gestational ages as well as neonatal pups for the analysis of p19^{INK4d} expression in the forebrain, Sprague Dawley rats were mated overnight in the colony, which we maintain. The day of conception, detected by the presence of a vaginal plug, was considered to be embryonic day 0 (E0). Birth usually occurred on the 21st or 22nd day of gestation. To normalize the ages of the postnatal animals examined, E22 was considered equivalent to postnatal day 0 (P0).

To label replicating cells in the embryonic telencephalon between E14 and E20, as well as in the P0–P2 SVZa and RMS thymidine analog used as a cell proliferation marker BrdU was administered intraperitoneally (200 mg/kg) to pregnant dams. The BrdU was administered 45 min or 3, 4, or 9 hr before perfusion to visualize labeled cells in different positions of the VZ as they undergo interkinetic nuclear migration. Timed embryos were removed from the uterus of pregnant dams that were deeply anesthetized with chloral hydrate (350 mg/kg) and perfused transcardially with cold 4% paraformaldehyde in 0.1 M PBS, pH 7.4. The P0–P2 pups were also administered BrdU after anesthetization by ether inhalation, 3 or 9 hr before they were again anesthetized and perfused with 4% paraformaldehyde. The perfused brains of both the embryonic and neonatal rats were removed from the skull, post-fixed overnight at 4°C in the same fixative, and cryoprotected with 20% sucrose for 24 hr. All brains were embedded in O.C.T. (Miles, Elkhart, IN), frozen with liquid nitrogen, cut in the sagittal plane on a cryostat at 10 μm, and then mounted onto Superfrost(plus) slides (Fisher Scientific, Houston, TX).

Immunohistochemical procedures. The immunohistochemical detection of p19^{INK4d}, neuron-specific type III β-tubulin (detected by the antibody referred to as TuJ1), and BrdU was performed on the brains of at least three rats examined at E14, E15, E16, E18, E20, P0, and P2. For some analyses, we modified a previously described procedure from Menezes et al. (1995) to double-label sections with anti-p19^{INK4d} and TuJ1 or either antibody alone. Sections were rinsed in 0.1 M PBS, pH 7.4, and kept in blocking serum (1.5% normal goat serum and 0.01% Triton X-100 in 0.1 M PBS, pH 7.4) for 1 hr. Subsequently, the sections were incubated overnight at 4°C in anti-p19^{INK4d} (Santa Cruz Biotechnology, Santa Cruz, CA) or TuJ1 (Promega, Madison, WI) at 1:100 and 1:400 dilutions, respectively, or a combination of anti-p19^{INK4d} and TuJ1 with the same final dilutions. The following day the sections were rinsed with PBS and incubated, at room temperature, in the appropriate secondary antibodies or antibody (Jackson ImmunoResearch, West Grove, PA) added to blocking serum at a 1:200 final dilution. For consistency we always used fluorescein-conjugated goat anti-rabbit IgG for detection of the anti-p19^{INK4d} and rhodamine-conjugated goat anti-mouse for visualization of the TuJ1. For double-labeling, cocktails of secondary antibodies were added to blocking serum at 1:200 final dilution and applied to the sections. After a 1 hr incubation, the sections were washed with PBS and coverslipped with Vectashield (Jackson ImmunoResearch).

An adjacent set of sections to those used for the p19^{INK4d}/TuJ1 labeling was used to reveal BrdU immunoreactivity in sections also stained with anti-p19^{INK4d}. For the detection of BrdU-labeled cells, the sections were rinsed in 0.1 M PBS, immersed in 2N hydrochloric acid (HCl) at 40°C for 20 min to denature the DNA, and then rinsed twice with 0.1 M borate buffer, pH 8.4, for 15 min to neutralize the HCl. After several PBS washes, the sections were immersed in blocking serum for 1 hr and then incubated overnight at 4°C in a combination of rat monoclonal anti-BrdU (Accurate Chemicals, Westbury, NY) and anti-p19^{INK4d} added to blocking serum at a 1:400 and 1:100 final dilution, respectively. The next day, the sections were rinsed with PBS and incubated for 1 hr at room temperature in a cocktail of the appropriate secondary antibodies (fluorescein-conjugated goat anti-rabbit IgG for anti-p19^{INK4d} and rhodamine-conjugated goat anti-rat for anti-BrdU). Both secondary antibodies were added to blocking serum at a 1:200 final dilution. After the secondary antibody incubation, sections were washed with PBS and coverslipped with Vectashield. To demonstrate the specificity of labeling, the primary antibodies were omitted in the control sections in all stainings.

To distinguish cytoarchitectural features, chosen sections neighboring those stained for p19^{INK4d} were stained with cresyl violet (CV). Briefly, after incubation in a series of descending alcohol concentrations and then xylene, the sections were stained with CV (0.5%) for 30 min. Sections were examined using a Zeiss Axioscope fluorescence microscope or a confocal Zeiss Axioplan equipped with LSM 510. Confocal images were obtained from a single optical section with a thickness of 1 μm. The laser scanning at 488 nm (for fluorescein) and 543 nm (for rhodamine) was performed sequentially to avoid bleed-through of the separate fluorescent signals. The captured images were merged and processed using Adobe Photoshop.

RESULTS

We studied the regulation of the proliferation and differentiation of cells in the embryonic telencephalon and neonatal RMS by analyzing the pattern of expression of the CDKI p19^{INK4d} by the cells of the prenatal and postnatal forebrain. To determine whether and which cells have initiated differentiation, on the basis of their expression of p19^{INK4d} and neuron-specific tubulin, rat embryos and pups were administered the cell proliferation marker BrdU at various times before their perfusion, and subsequently the brains of these animals were immunostained with p19^{INK4d} and anti-BrdU, as well as the neuron-specific antibody TuJ1, which recognizes neuron-specific type III β-tubulin. p19^{INK4d} was chosen for analysis because of its governing role in determining whether a cell in the developing CNS continues to divide or withdraw from the cell cycle. Recent data suggest that p19^{INK4d} not only regulates cell cycle exit at the G_1 phase but also plays a role in maintaining cells in the postmitotic state (Zindy et al., 1999). The state and phenotype of differentiation of the cells in the embryonic telencephalon and RMS were determined by double-labeling sections with an antibody to p19^{INK4d} and with the antibody TuJ1 (Lee et al., 1990; Easter et al., 1993).

The spatiotemporal expression pattern of p19^{INK4d} in the developing cerebral cortex of rats was examined between E14 and E20, during which time the majority of the neurons of the cerebral cortex are generated. During embryonic development, the cerebral cortex expands from the VZ, a pseudostratified neuroepithelium surrounding the lateral ventricles, to a multilayered laminar structure. The progenitors of the VZ, which undergo interkinetic nuclear migration, divide at the ventricular surface and generate immature neurons after withdrawing from the cell cycle. In contrast to the VZ cells, the progenitor cells of the SVZ essentially divide at the same place where they synthesize their DNA. In an orderly manner, the newly generated postmitotic neurons migrate away from the VZ (or overlying SVZ), usually along radial glia, to their final destinations in the cortical plate (Fig. 1) (Edmondson and Hatten, 1987). The earliest-generated neurons of the telencephalon form the preplate, which subsequently becomes subdivided into the marginal zone and subplate by the insertion of the later-generated neurons destined for the cortical plate.

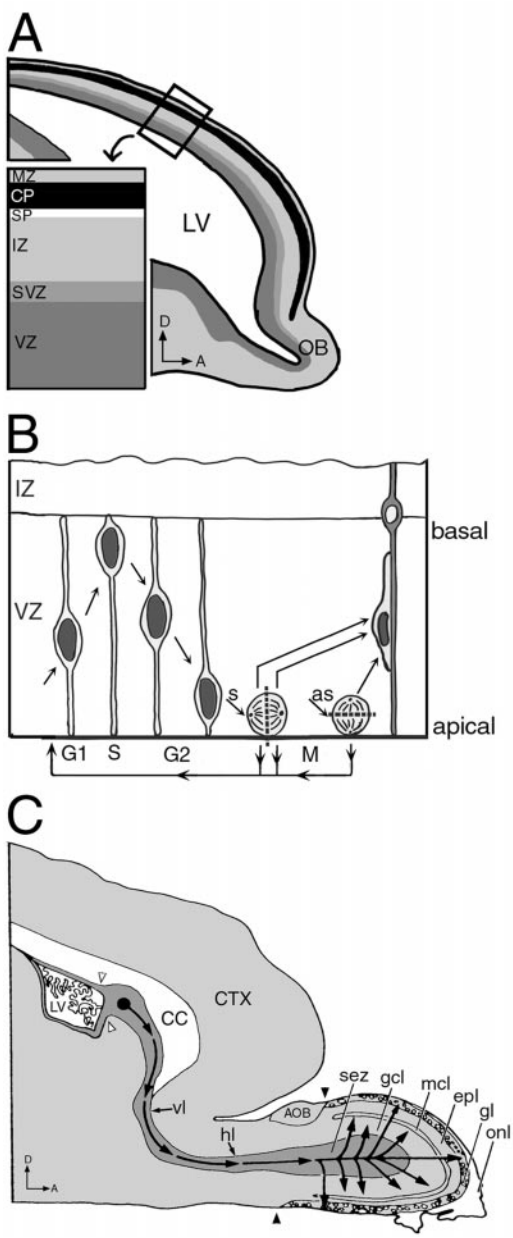

Figure 1. The generation of forebrain neurons by progenitor cells of the embryonic and neonatal telencephalon. *A*, Diagram of a sagittal view of the rat embryonic telencephalon showing the laminar subdivisions of the developing cerebral cortex. The progenitor cells of the telencephalon reside in the ventricular zone that lines the lateral ventricles and in the overlying subventricular zone. The *boxed area* indicates the approximate region of the dorsal telencephalon that was analyzed in all age groups and shown at higher magnification in the *inset*. Postmitotic neurons generated in the VZ and SVZ migrate through the intermediate zone and subplate to reach their destinations in the cortical plate. The subplate and marginal zone contain the earliest-generated neurons of the telencephalon. *B*, Schematic drawing depicting the process of interkinetic nuclear migration and the symmetric and asymmetric division of telencephalic progenitor cells of the ventricular zone and a portion of the overlying intermediate zone. During interkinetic nuclear migration the progenitor cells extend processes to both the apical and basal borders of the VZ, and the nuclei translocate from the apical to the basal border of the VZ; each position of the nuclei correlates with a different phase of the cell cycle. While in the G_1 phase of the cell cycle, nuclei move from the ventricular surface toward the intermediate zone or basal border. Most of the progenitor cell nuclei located along the basal border of the VZ are in the S phase of the cell cycle, during which DNA synthesis occurs. In the G_2 phase of the cell cycle, the nuclei return to the ventricular surface, retract their processes, and undergo cell division during the M phase of the cell cycle. An individual progenitor cell can divide asymmetrically, denoted by the *arrow* labeled *as* and a *horizontal dashed line* separating the spindle apparatus. In the *illustration* shown, the daughter cell adjacent to the ventricular lining continues to proliferate in the VZ, and the other daughter cell becomes a postmitotic neuron and then begins to migrate toward the pia usually in association with a radial glial fiber. Alternatively, a cell can undergo symmetric division, denoted by the *arrow* labeled *s* and a *vertical dashed line* in the *middle* of the spindle apparatus. After symmetric division, both daughter cells either go through another round of interkinetic nuclear migration or exit the cell cycle as depicted by the *pair* of *arrows*. *C*, Diagram of a sagittal view of the neonatal forebrain showing the site of origin, path of migration, and site of destination of neurons arising in the SVZa. The SVZa neuronal progenitor cells are located within a distinct region of the anterior part of the postnatal subventricular zone of the forebrain represented by a *filled circle* in the center of the SVZa. SVZa-derived cells migrate along a highly restricted pathway, the rostral migratory stream (RMS), to reach the subependymal zone in the middle of the olfactory bulb and then migrate radially to one of the overlaying cellular layers of the olfactory bulb, where they differentiate into interneurons of the granule cell and glomerular layers. The set of *open arrowheads* (close to the lateral ventricle) demarcates the border between the region of the SVZa and the posterior portion of the SVZ that generates predominantly glia. The rostrally placed set of *filled arrowheads* denotes the caudal border of the olfactory bulb. *A*, Anterior; *AOB*, accessory olfactory bulb; *CC*, corpus callosum; *CP*, cortical plate; *CTX*, cerebral cortex; *D*, dorsal; *epl*, external plexiform layer; *gcl*, granule cell layer; *gl*, glomerular layer; *hl*, horizontal limb of the RMS; *IZ*, intermediate zone; *LV*, lateral ventricle; *mcl*, mitral cell layer; *MZ*, marginal zone; *OB*, olfactory bulb; *onl*, olfactory nerve layer; *sez*, subependymal zone; *SP*, subplate; *SVZa*, anterior part of the neonatal subventricular zone; *vl*, vertical limb of the RMS; *VZ*, ventricular zone.

We also analyzed the expression pattern of $p19^{INK4d}$ by the cells of the RMS, the pathway traversed by the mitotic progeny of cells located within a distinct region of the anterior part of the postnatal subventricular zone of the forebrain designated the SVZa. After the SVZa-derived cells reach the olfactory bulb, they permanently cease division and differentiate into interneurons of the granule cell and glomerular layers of the olfactory bulb. SVZa neuronal progenitor cells possess a unique mitotic capacity compared with the progenitor cells of the rest of the telencephalon and other regions of the developing CNS. One distinguishing feature is that the SVZa and SVZa-derived cells in the RMS continue to proliferate throughout life. Unlike the progenitor cells of the embryonic telencephalic VZ, SVZa progenitors initiate differentiation without becoming postmitotic, such that proliferation and differentiation occur concurrently. In addition, on the basis of their phenotypic characteristics, they are full-fledged neurons, but they retain the ability to undergo division as they migrate, although the extent of mitosis steadily decreases as the cells approach the olfactory bulb (Menezes et al., 1995; Smith and Luskin, 1998). To investigate what accounts for the ability of SVZa neuronal progenitor cells to divide as they migrate, $p19^{INK4d}$ was analyzed because of its pivotal role in regulating the mechanisms of the cell cycle.

Spatiotemporal pattern of $p19^{INK4d}$ expression in the developing telencephalon

The developing telencephalon was analyzed to characterize the expression pattern of $p19^{INK4d}$ during cortical neurogenesis (E14–E20). By correlating the positions of cells as they undergo interkinetic nuclear migration with their stage of the cell cycle and pattern of $p19^{INK4d}$ expression, our data suggest that the VZ can be further subdivided into a sublamina in which the majority of the cells are $p19^{INK4d}(+)$ and a sublamina in which the

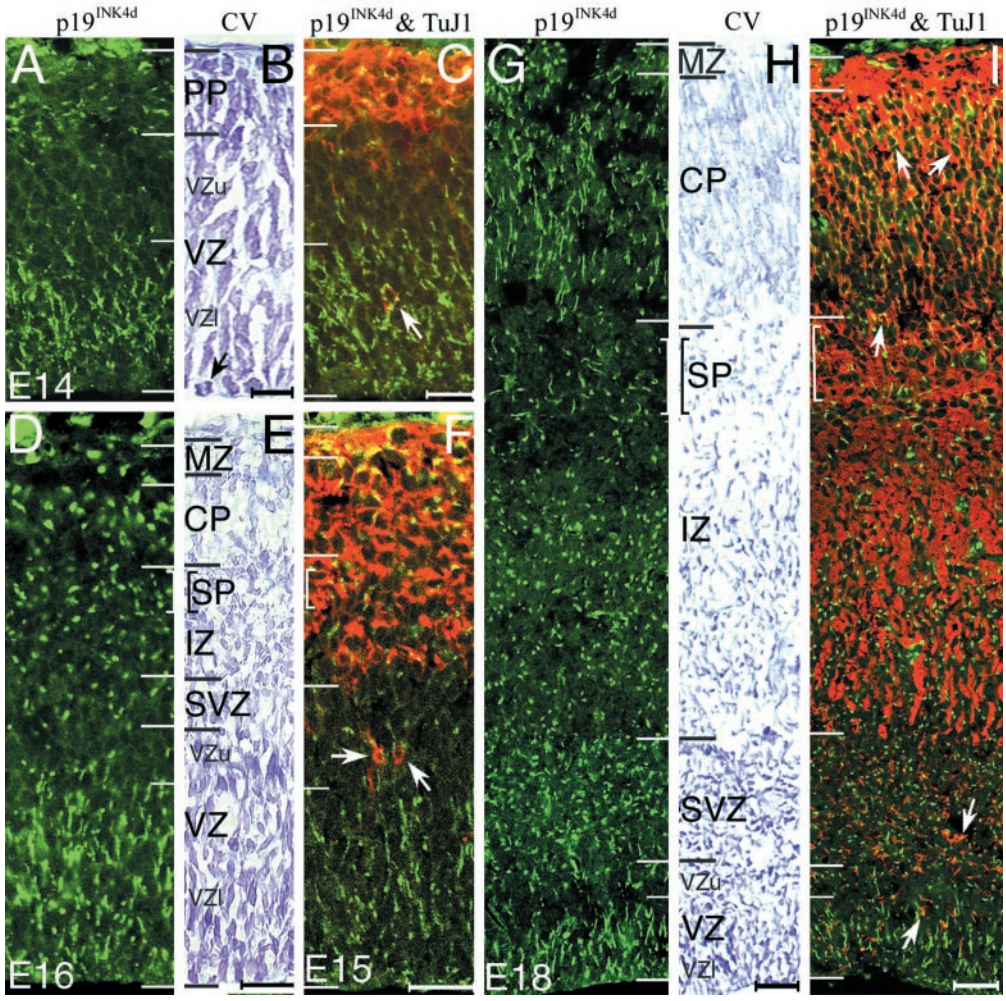

Figure 2. Spatiotemporal pattern of p19^{INK4d} and neuron-specific type III β-tubulin expression in the embryonic telencephalon. *A–I*, Fluorescent photomicrographs of representative parasagittal sections were obtained by confocal microscopy from the dorsal part of the telencephalon at E14 (*A, C*), E15 (*F*), E16 (*D*), and E18 (*G, I*) and stained with anti-p19^{INK4d} (recognized by a fluorescein-conjugated secondary antibody) and the neuron-specific antibody TuJ1 (recognized by a rhodamine-conjugated secondary antibody). Neighboring sections were stained with cresyl violet (*B, E, H*) to demonstrate the corresponding laminae of the developing cerebral cortex. *A–C,* At E14, on the basis of the pattern of p19^{INK4d} immunoreactivity, the VZ can be divided into a p19^{INK4d}(+) sublamina in the lower (apical) portion of the VZ [VZ lower (*VZl*)] and a p19^{INK4d}(−) sublamina in the upper (basal) portion of the VZ [VZ upper (*VZu*)]. The VZl is a mixture of cells at different stages of the cell cycle, including cells undergoing cytokinesis along the ventricular surface (e.g., *B*, *arrow*), progenitor cells that are in the G_1 phase of the cell cycle, and newly generated postmitotic neurons. Immature neurons that have recently exited the cell cycle are most likely the p19^{INK4d}-expressing cells of the VZl. In the VZu, which contains progenitor cells that are in the S phase of the cell cycle and migrating immature postmitotic neurons, there is a low level of p19^{INK4d} immunoreactivity. This indicates that the cells in the VZu, undergoing DNA synthesis, are primarily devoid of p19^{INK4d} immunoreactivity. In contrast to the differential pattern of p19^{INK4d} staining in the sublaminae of the VZ, the staining with TuJ1 is minimal in both the VZu and VZl. The few p19^{INK4d}(+)/TuJ1(+) cells in the VZ most likely represent newly generated postmitotic neurons destined for the cortical plate (*C*, *arrow*). In addition, postmitotic cells of the preplate, which contains the future Cajal Retzius and subplate cells, are also labeled by anti-p19^{INK4d}. *D–I*, As development proceeds from E14 to E18, the VZ becomes thinner, and the overlying SVZ becomes thicker. Similar to the telencephalon at E14 (*A–C*), at E15 and E16 (*D–F*), and at E18 (*G–I*) the VZu is predominantly a p19^{INK4d}(−) sublamina, and the VZl is a p19^{INK4d}(+) sublamina. However, at progressively older ages, the VZu/VZl ratio becomes smaller (i.e., a greater proportion of VZ is comprised of the VZl). Note the uniform and prominent distribution of p19^{INK4d} expression by cells of the SVZ. In addition, at E15 (*F*) and E18 (*I*), many p19^{INK4d} (+) neurons of the cortical plate, subplate, intermediate zone, and marginal zone are also immunoreactive for TuJ1 (i.e., *arrows*). Note that the p19^{INK4d} expression by the postmitotic immature neurons in the VZu appears to be downregulated. After reaching the intermediate zone, the p19^{INK4d} expression by TuJ1(+) immature neurons appears to be activated again. Also, note that the perinuclear p19^{INK4d} staining pattern is more extensive in the neurons of the cortical plate than in those of the subplate and intermediate zone where the p19^{INK4d} has a punctuate perinuclear distribution (also see Fig. 4). *CP*, Cortical plate; *CV*, cresyl violet; *IZ*, intermediate zone; *MZ*, marginal zone; *PP*, preplate; *SP*, subplate; *SVZ*, subventricular zone; *VZ*, ventricular zone. Scale bars: *A–C*, 20 μm; *D–I*, 50 μm.

majority of the cells are p19^{INK4d}(−) (Fig. 2). The p19^{INK4d}(+) sublamina is situated in the apical portion of the VZ, adjacent to the ventricle, referred to as VZ lower (or abbreviated VZl). Interestingly there is a sharp boundary between the VZl and the VZ upper (VZu), which would not be predicted by the process of interkinetic nuclear migration. The particular environmental influences that presumably set up the boundary have not been determined. However, from BrdU and tritiated-thymidine studies (Brand and Rakic, 1979), one can conclude that the VZl contains newly generated postmitotic neurons that have just withdrawn from the cell cycle as well as cells at different stages of the mitotic cycle, including progenitor cells undergoing cytokinesis along the ventricular surface and cells in the G_1 phase. Moreover, our recognition that the VZ is a bilaminar structure, on the basis of its

p19INK4d-staining pattern combined with our previous knowledge from the literature of the kinetics of the VZ cells, suggested to us that the cells are expressing p19INK4d in the VZl are most likely immature neurons that have withdrawn recently from the cell cycle. Alternatively, we cannot exclude the possibility that the daughter cells destined to initiate a new round of interkinetic nuclear migration temporarily express p19INK4d (see below).

The other subdivision of the VZ revealed by its p19INK4d expression is the p19INK4d(−) sublamina in the basal or upper half of the VZ or VZu (Fig. 2). The VZu, like the VZl, is also a mixture of cells in different stages of the cell cycle, including progenitor cells going through, entering, or leaving S phase. In addition, the VZu is also comprised of immature neurons that are beginning their ascent to the cortical plate. The relatively low numbers of p19INK4d-expressing cells in the VZu may partly be because the cells do not express p19INK4d while they are actively undergoing DNA synthesis. The relatively few p19INK4d(+) cells in the VZu probably represent the postmitotic migrating neurons that withdrew recently from the cell cycle in the VZl and are en route to the cortical plate. In addition, to account for the low fraction of p19INK4d(+) cells in the VZu, we hypothesized that the postmitotic neurons traversing the VZu may temporarily downregulate their expression of p19INK4d on the basis of the observation that the VZu is flanked by the p19INK4d(+) VZl and the p19INK4d-immunoreactive intermediate zone. Evidence of this conjecture is given below.

As the neurogenesis of the cerebral cortex proceeds, the VZ becomes thinner and is completely depleted by the time all of the cortical neurons have been generated (approximately E20). However, as long as the cells of the VZ are undergoing proliferation, it has a bilaminar pattern of p19INK4d expression (Fig. 2). Furthermore, although the overall thickness of the VZ becomes smaller as cortical neurogenesis proceeds, we observed that the ratio of the thickness of VZu/VZl decreases. In other words, proportionally the p19INK4d(−) VZu becomes thinner and the p19INK4d(+) VZl becomes thicker (Fig. 2). The subventricular zone overlying the VZ, thought to be comprised of progenitor cells that undergo cytokinesis in the same position where they synthesize their DNA, also contains p19INK4d(+) cells. These p19INK4d(+) cells may represent newly generated neurons or glia that arise from the SVZ or cells traversing the SVZ destined for the cortical plate. In addition to the expression of p19INK4d by the postmitotic cells of the VZl, we observed that the postmitotic cells of the intermediate zone, cortical plate, and marginal zone also express p19INK4d. Furthermore, after the VZ is depleted of its cells, the part of the overlying SVZ that generates glia (posterior to the SVZa) also contains p19INK4d(+) cells.

Expression of p19INK4d by postmitotic neurons of the developing cerebral cortex

To determine more precisely when after cytokinesis newly generated neurons begin to express the cell cycle inhibitor p19INK4d, we examined the relationship between the pattern of expression of p19INK4d and that of neuron-specific type III β-tubulin, one of the earliest markers of immature neurons. We demonstrated previously that some immature neurons of the embryonic telencephalic VZ start to express neuron-specific type III β-tubulin (recognized by the antibody TuJ1) shortly after they exit the cell cycle in the VZ (Menezes and Luskin, 1994). Similarly, in this study, we noted a low number of TuJ1(+) cells in the VZ, which however increases over time (Fig. 2). When we stained sections of the embryonic telencephalon with TuJ1, in conjunction with anti-p19INK4d, we observed that the vast majority of TuJ1(+) cells in the VZ as well as in SVZ were also p19INK4d(+), indicating that p19INK4d is indeed expressed by the postmitotic neurons of the developing cerebral cortex. We noted, however, that higher levels of p19INK4d were expressed by the TuJ1(+) cells of the intermediate zone, cortical plate, and marginal zone (Fig. 2), which indicates that type III β-tubulin and p19INK4d both persist and are expressed more intensely by the more mature neurons of the developing cerebral cortex.

To address the question of whether the progeny of a given progenitor cell express p19INK4d at the moment of their withdrawal from the cell cycle, we administered the cell proliferation marker BrdU to embryos aged E14–E20 45 min or 3 hr, 4 hr, or 9 hr before their perfusion and then compared the single-labeled [BrdU(+)/p19INK4d(−)] with the double-labeled [BrdU(+)/p19INK4d(+)] cells. Shorter BrdU exposure times (i.e., 45 min) allowed us to identify the VZ progenitor cells that are in the process of migration from the VZu (site of DNA synthesis and BrdU incorporation) to the ventricular surface, before mitosis (Fig. 3*A*). When we stained the developing telencephalon with antibodies to p19INK4d and BrdU and analyzed the superficial portion of the VZl 3 hr after BrdU, we observed BrdU(+) cells, but we did not detect double-labeled cells (Fig. 3*D*), indicating that the progenitor cells that synthesized their DNA and were moving to the VZ surface during their G_2 phase do not express p19INK4d. We also examined whether the cells were single- and double-labeled in the VZ 9 hr after BrdU. The administration of BrdU to embryos at such a relatively long time period before their perfusion (i.e., 9 hr) revealed both BrdU(+)/p19INK4d(−) and BrdU(+)/p19INK4d(+) populations of cells in the superficial portion of the VZl (Fig. 3*E*). Our interpretation is that the BrdU(+)/p19INK4d(−) cells are the progenitor cells that took up BrdU at later time points and are moving toward the ventricular surface. On the other hand, the BrdU(+)/p19INK4d(+) cells are presumably the immature neurons migrating to the cortical plate whose ancestors incorporated BrdU at earlier time points and had enough time to migrate down to the VZ, undergo mitosis, and subsequently begin to migrate toward the cortical plate. These conclusions are consistent with the studies that showed a 12–16 hr cell cycle length for the VZ progenitors during cortical neurogenesis (Takahashi et al., 1995). Our results argue that the p19INK4d is expressed by the progeny of the VZ progenitors at the actual time of withdrawal from the cell cycle at the ventricular surface.

Changes in subcellular distribution of p19INK4d in the cells of the developing telencephalon

To determine whether the subcellular distribution of p19INK4d in postmitotic cortical neurons is related to their state of differentiation as they proceed from the VZ to the cortical plate, we analyzed the intracellular localization of p19INK4d in TuJ1(+) cells. As shown above and described previously (Menezes and Luskin, 1994), the postmitotic immature neurons begin to express type III β-tubulin in the VZ presumably immediately after undergoing cytokinesis. The neuron-specific tubulin is expressed throughout the soma and gradually becomes more intense as cells differentiate and migrate through the intermediate zone to the overlying layers of the developing cortex. In contrast to the expression of type III β-tubulin, we observed that not only does the intensity of p19INK4d increase but the subcellular distribution of p19INK4d also changes as cells undergo progressive differentiation during their ascent from the VZ to the cortical plate. Furthermore, although TuJ1 stains the entire soma, p19INK4d

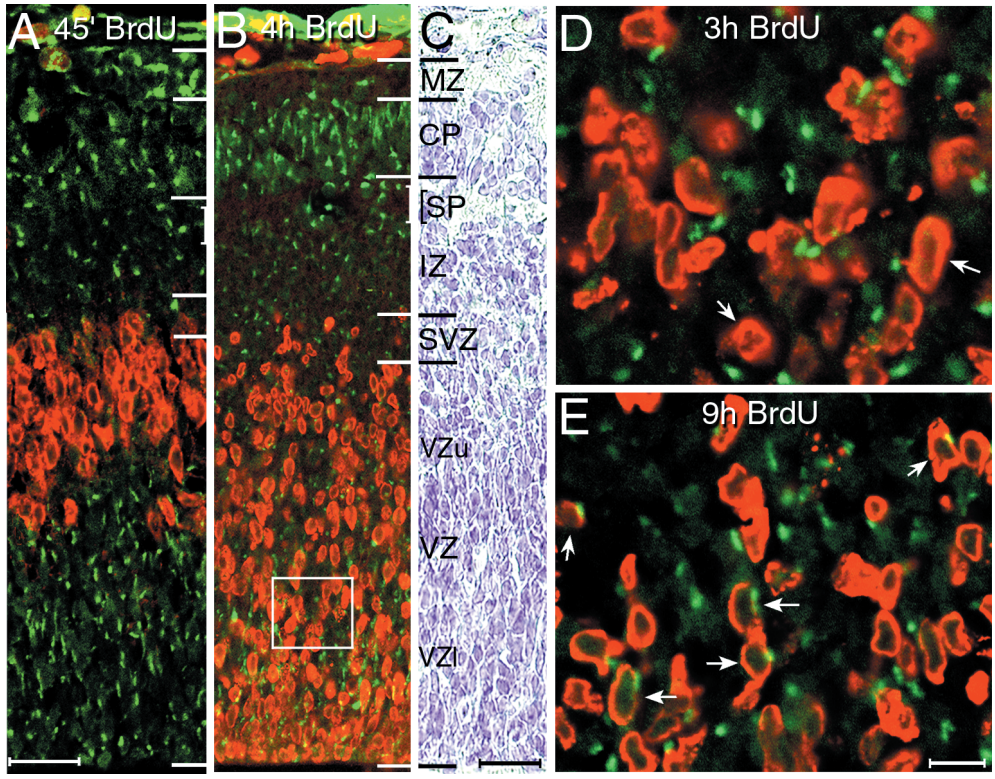

Figure 3. Expression pattern of p19^{INK4d} by telencephalic VZ cells as a function of their phase of the cell cycle. *A–C*, Photomicrographs of the distribution of the BrdU(+) cells in parasagittal sections of the dorsal part of the E16 telencephalon from embryos perfused 45 min (*A*) and 4 hr (*B*) after BrdU administration. The sections were stained with an antibody to p19^{INK4d} (*green*) and to BrdU (*red*). Forty-five minutes after the administration of BrdU, the BrdU(+) cells are located in the VZu (*A*), whereas after 4 hr the BrdU(+) cells are distributed throughout the VZ but are concentrated in the VZl (*B*). This labeling pattern demonstrates that as the cells of the VZ undergo interkinetic nuclear migration, some nuclei that incorporated BrdU move from the VZu to the VZl within 4 hr. *C*, an adjacent section to *B*, is stained with cresyl violet to show the lamination in a corresponding part of the telencephalon. The *boxed area* in *B* indicates the approximate region of the VZl shown at higher magnifications in *D* and *E*. *D, E*, Representative confocal photomicrographs from the superficial portion of the E16 VZl double-labeled with an antibody to p19^{INK4d} (*green*) and an antibody to BrdU (*red*). The distribution of labeled cells in the telencephalic VZ was analyzed 3 hr (*D*) and 9 hr (*E*) after a pulse of BrdU. Three hours after the BrdU administration there were numerous BrdU(+) cells in the superficial portion of the VZl (*D*), which are probably migrating to the ventricular surface before undergoing mitosis. Note that these BrdU(+) cells do not express p19^{INK4d} (e.g., *D*, *arrows*). In contrast, *E* shows the labeling pattern in the superficial portion of the VZl 9 hr after a pulse of BrdU. It contains both BrdU(+)/p19^{INK4d}(−) and BrdU(+)/p19^{INK4d}(+) cells (e.g., *E*, *arrows*). As in *D*, the cells that incorporated BrdU recently and are en route to the VZl are probably the BrdU(+)/p19^{INK4d}(−) cells. By analogy, the double-labeled cells are probably ascending to the intermediate zone after undergoing division at the ventricular lining subsequent to incorporating BrdU in the VZu. In the double-labeled cells, the p19^{INK4d} has a perinuclear distribution as described in Figure 2, unlike the more dispersed staining present in p19^{INK4d}(+) cortical plate neurons. *BrdU*, Bromodeoxyuridine; *CP*, cortical plate; *IZ*, intermediate zone; *MZ*, marginal zone; *SP*, subplate; *SVZ*, subventricular zone; *VZ*, ventricular zone; *VZl*, lower portion of the ventricular zone; *VZu*, upper portion of the ventricular zone. Scale bars, *A–C*, 50 μm; *D, E*, 10 μm.

immunoreactivity was always more restricted to the cytoplasmic–nuclear border.

We detected layer-specific changes in the expression of p19^{INK4d} by cells of the developing cerebral cortex, suggesting that p19^{INK4d} is dynamically regulated. Initially, when the progeny of the progenitor cells in the VZl withdraw from the cell cycle, most of the postmitotic cells express p19^{INK4d} outlining the cytoplasmic–nuclear border in the apical half of the cell in a crescent shape (Fig. 2). In the VZu, we observed lower levels of p19^{INK4d} immunoreactivity than in the VZl or overlying intermediate zone, suggesting that cells traversing the VZu may downregulate their expression of p19^{INK4d} (Fig. 2). As the immature neurons migrating through the intermediate zone start to reexpress the p19^{INK4d}, the p19^{INK4d} immunoreactivity no longer appears to form a crescent around the nucleus but becomes more restricted in its distribution. It is still localized to the cytoplasmic–nuclear border, but in a punctate manner (Figs. 2, 4). The intracellular distribution of p19^{INK4d} undergoes another change as the cells enter the cortical plate and become more differentiated. p19^{INK4d} again caps the apical half of the nucleus but appears more intense than in the VZl (Figs. 2, 4). The mechanism(s) that regulates the highly orchestrated series of changes in the intracellular localization of the p19^{INK4d} has not been elucidated.

Spatiotemporal pattern of p19^{INK4d} expression along the rostral migratory stream

We examined the spatiotemporal pattern of p19^{INK4d} expression in the neonatal (P0–P2) rat forebrain and, in particular, in and around the RMS to find out when and where the SVZa-derived cells, which traverse the pathway, express the cell cycle inhibitor p19^{INK4d}. We observed a gradient of p19^{INK4d} expression in the RMS (Fig. 5), such that as the progenitor cells originating in the SVZa migrate toward the subependymal zone in the center of the olfactory bulb, they express increasingly higher levels of p19^{INK4d}. Furthermore, the number of cells expressing p19^{INK4d}

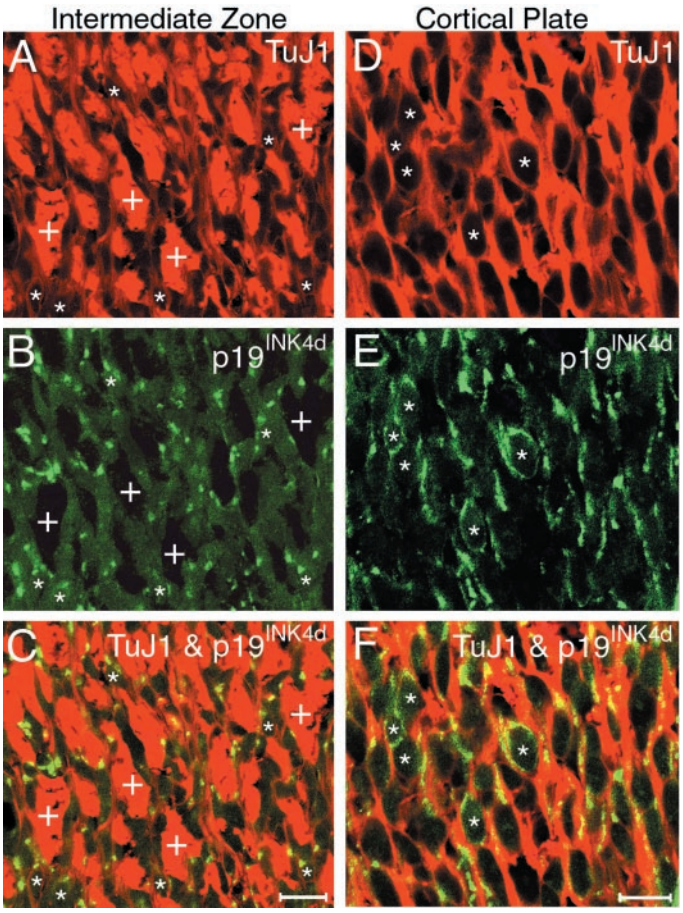

Figure 4. Discrete perinuclear localization of p19^{INK4d} expression by cortical plate neurons compared with the punctate distribution of p19^{INK4d} labeling of the neurons traversing the intermediate zone. *A–F*, Fluorescent confocal photomicrographs of representative sections of the E18 intermediate zone (*A–C*) and cortical plate (*D–F*) stained with the neuron-specific antibody TuJ1 (*red*) and anti-p19^{INK4d} (*green*). The confocal images captured with the rhodamine filter (*A, D*) and fluorescein filter (*B, E*) are superimposed in *C* and *F*, respectively. Nuclei of identical double-labeled cells are indicated by *asterisks* in *A–C* or in *D–F*. The anti-p19^{INK4d} labeling (*green*) is restricted to the cytoplasmic–nuclear border in the apical part of the cortical neurons, whereas TuJ1 stains the entire soma. Note that p19^{INK4d} has a punctate pattern of expression in the intermediate zone (*A–C*), whereas p19^{INK4d} labeling of the cortical plate neurons is more extensive and appears to cap the nucleus (*D–F*). Furthermore, the axonal bundles of the intermediate zone (*A–C*, *crosses*) are TuJ1 immunoreactive and devoid of p19^{INK4d} staining. Note the presence of punctate p19^{INK4d} staining, primarily localized to the apical pole of neurons adjacent to the axonal bundles. Scale bars: *A–F*, 10 μm.

becomes greater along the RMS from the SVZa to the subependymal zone. The increase in the density of p19^{INK4d}(+) cells, however, is not linear; rather it is most pronounced at the transition from SVZa to the vertical limb of the RMS (Fig. 5). The p19^{INK4d} expression persists in the olfactory bulb in the permanently postmitotic SVZa-derived cells of the granule cell and glomerular layers, as well as in the earlier-generated neurons of the mitral cell layer of the olfactory bulb. Furthermore, the relatively quiescent ependymal cells that line the lateral ventricles showed significantly higher levels of p19^{INK4d} expression in comparison with that of the subjacent SVZa cells (Figs. 5, 6). This pattern of p19^{INK4d} staining of the ependyma and RMS is the inverse of the gradient of actively dividing cells. Accordingly, in the RMS we observed a stepwise reduction in the extent of BrdU incorporation along the RMS, minimal incorporation of BrdU in the subependymal zone in the middle of the olfactory bulb, and negligible labeling of the ependymal cells lining the lateral ventricles (Fig. 5). Our p19^{INK4d} findings in conjunction with those from our BrdU studies demonstrate that an increasing proportion of the SVZa-derived cells withdraw from the cell cycle as they approach the olfactory bulb.

Expression of p19^{INK4d} by the neuronal progenitor cells of the rostral migratory stream and their progeny

To determine how the spatiotemporal expression pattern and intracellular distribution of p19^{INK4d} correlate with the phenotype, proliferative activity, and stage of differentiation of the cells in the RMS, we compared the pattern of p19^{INK4d} expression with that of neuron-specific type III β-tubulin using immunocytochemistry. In this study, we confirmed our previous results that virtually all the cells along the RMS are immunoreactive for the neuron-specific antibody TuJ1 (Menezes et al., 1995). Furthermore, as expected from the pattern of TuJ1 staining and role of p19^{INK4d}, we did not detect p19^{INK4d}(+)/TuJ1(+) cells in the SVZa (Fig. 6). However, there was a pronounced gradient in the RMS of double-labeled cells as the olfactory bulb was approached; regions closer to the olfactory bulb expressed a higher proportion of p19^{INK4d}(+)/TuJ1(+) cells. In fact the majority of the cells in the horizontal limb of the RMS coexpress p19^{INK4d} and type III β-tubulin. Moreover, although most cells in the subependymal zone of the olfactory bulb were also double-labeled, they showed a greater intensity of staining for both p19^{INK4d} and type III β-tubulin. We also detected a low fraction of cells that were TuJ1(+) but p19^{INK4d}(−) in addition to the double-labeled cells in the RMS, suggesting that some cells destined for the olfactory bulb may downregulate their p19^{INK4d} expression to undergo subsequent rounds of cell division (see below).

Although nearly all of the cells of the RMS express p19^{INK4d}, we examined whether the intracellular distribution of p19^{INK4d} changes as a function of the phase of the cycle and/or the state of differentiation of a cell, as was found to be the case in the developing cerebral cortex. We found that p19^{INK4d} was expressed at the cytoplasmic–nuclear border of the cells all along the RMS (Figs. 5, 6), just as in the p19^{INK4d}-expressing cells of the different layers of developing cerebral cortex (Figs. 2, 4). However, in contrast to the developing cerebral cortex, in the cells of the RMS the p19^{INK4d} was always expressed in a punctate manner both in dividing as well as in the postmitotic cells. Furthermore, in most cells of the RMS, the p19^{INK4d} immunoreactivity was concentrated in the half of the cell closest to the leading process, similar to its distribution in immature neurons migrating toward the cortical plate. Collectively, these findings indicate that the SVZa-derived cells may regulate their expression of p19^{INK4d} differently from cells destined for the cerebral cortex.

To determine whether the p19^{INK4d}-expressing cells within the RMS undergo cell division, we administered an intraperitoneal injection of BrdU to neonatal pups and perfused them at various subsequent time points. We analyzed the distribution of p19^{INK4d}(+)/BrdU(+) cells as a function of the position of a cell along the anterior–posterior axis of the RMS. Because the length of the cell cycle of SVZa-derived cells is ~12 hr (Smith and Luskin, 1998), we perfused pups 3 hr after BrdU (while the proliferating cells were in S/G_2 phase) and 9 hr after BrdU (to give the cells sufficient time to incorporate BrdU and proceed

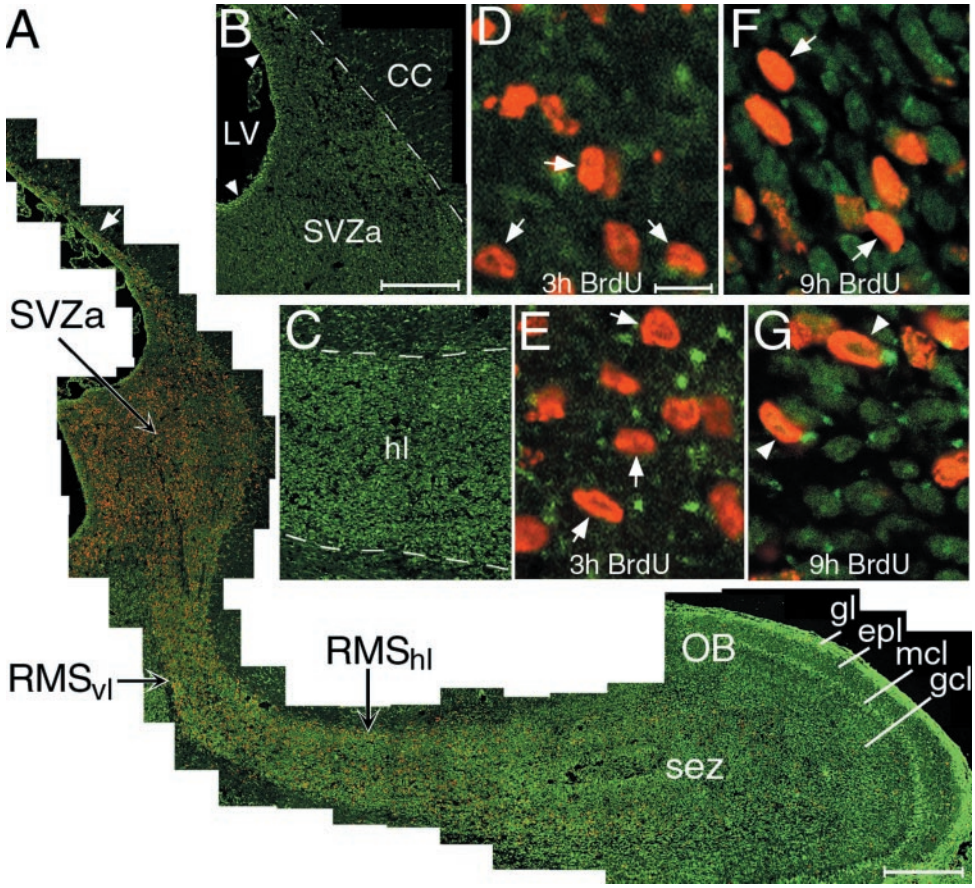

Figure 5. Gradient and subcellular distribution of p19^{INK4d} and BrdU immunoreactivity in the neonatal anterior subventricular zone (*SVZa*) and contiguous rostral migratory stream (*RMS*) after different post-BrdU intervals. *A*, A confocal photomontage of a sagittal section of the P2 forebrain illustrating the spatiotemporal distribution of BrdU(+) cells (*red*) and p19^{INK4d} expression (*green*) along the RMS from the SVZa to the subependymal zone in the middle of the olfactory bulb. An intraperitoneal injection of BrdU was given to a P2 rat pup 9 hr before its perfusion to demonstrate the distribution of mitotically active cells along the anterior–posterior axis of the RMS. The labeling pattern revealed by p19^{INK4d} immunoreactivity is the converse of that exhibited by the BrdU labeling. Specifically, in the SVZa the BrdU labeling is highest and the p19^{INK4d} immunoreactivity is lowest, whereas in the subependymal zone the p19^{INK4d} immunoreactivity is highest and the BrdU labeling is lowest. The *arrow* designates the division between SVZa and gliogenic posterior SVZ. *B, C*, High-magnification photomicrographs comparing the distribution of p19^{INK4d} immunoreactivity in the SVZa with that in the horizontal limb of the RMS. As described in *A*, the SVZa (*B*), with the exception of the ependymal layer (e.g., *arrowheads*), exhibits a low level of p19^{INK4d} immunoreactivity compared with that of the RMS (*C*). *D–G*, Fluorescent photomicrographs demonstrating the pattern of p19^{INK4d} and BrdU immunoreactivity in the SVZa (*D, E*) and horizontal limb of the RMS (*E, F*) 3 and 9 hr, respectively, after BrdU administration. Three hours (*D*) and 9 hr (*F*) after BrdU administration, the BrdU(+) neuronal progenitor cells in the SVZa do not coexpress p19^{INK4d} (*arrows*). However, 9 hr after the BrdU administration, many of the BrdU(+) cells in the horizontal limb of the RMS are also p19^{INK4d} immunoreactive (*G*, *arrowheads*), although 3 hr after BrdU the BrdU(+) cells were not labeled by p19^{INK4d} [i.e., BrdU(+)/p19^{INK4d}(−); *E*, *arrows*]. In the double-labeled BrdU(+)/p19^{INK4d}(+) cells, the p19^{INK4d} has a perinuclear distribution localized to the portion of the migrating SVZa-derived cells closest to the leading edge. The acquisition of p19^{INK4d} labeling in the horizontal limb of the RMS 9 hr after BrdU but not 3 hr after BrdU suggests that the SVZa-derived cells, which undergo multiple rounds of cell division as they migrate to the olfactory bulb, downregulate their p19^{INK4d} expression before proceeding through each subsequent round of division. *BrdU*, Bromodeoxyuridine; *CC*, corpus callosum; *epl*, external plexiform layer; *gcl*, granule cell layer; *gl*, glomerular layer; *hl*, horizontal limb of the RMS; *LV*, lateral ventricle; *mcl*, mitral cell layer; *OB*, olfactory bulb; *sez*, subependymal zone; *vl*, vertical limb of RMS. Scale bars: *A*, 300 μm; *B, C*, 100 μm; *D–G*, 10 μm.

through the M phase of the cell cycle). Because SVZa-derived cells migrate at 23 μm/hr (Luskin and Boone, 1994), we surmised that where we see BrdU(+) cells is probably relatively close to their site of proliferation; SVZa-derived cells cannot traverse more than a fraction of the pathway within 3 or 9 hr time intervals. An analysis of the distribution of labeled cells using confocal microscopy revealed the presence of BrdU(+)/p19^{INK4d}(−) cells in the SVZa 3 and 9 hr after BrdU administration (Fig. 5*D,F*). These data indicate that the neuronal progenitor cells in the SVZa undergo cell divisions without expressing p19^{INK4d}, unlike the immature neurons of the developing cerebral cortex. Conversely, the presence of BrdU(+)/p19^{INK4d}(+) cells in the horizontal limb of the RMS 9 hr after BrdU (Fig. 5*G*), but not 3 hr after BrdU (Fig. 5*E*), suggests that cells may downregulate their p19^{INK4d}, incorporate BrdU within the 9 hr interval after injection, and then reexpress p19^{INK4d} in the pathway.

DISCUSSION

By blocking the cell cycle at the G_1 phase, CDKIs and, in particular, p19^{INK4d} might couple proliferation arrest to the terminal differentiation of the cells in the developing CNS. To determine whether the progenitor cells of the telencephalic VZ differ in their cell cycle kinetics from that of the neonatal RMS, we characterized the spatiotemporal expression pattern of p19^{INK4d} in both progenitor cell populations. We showed that the

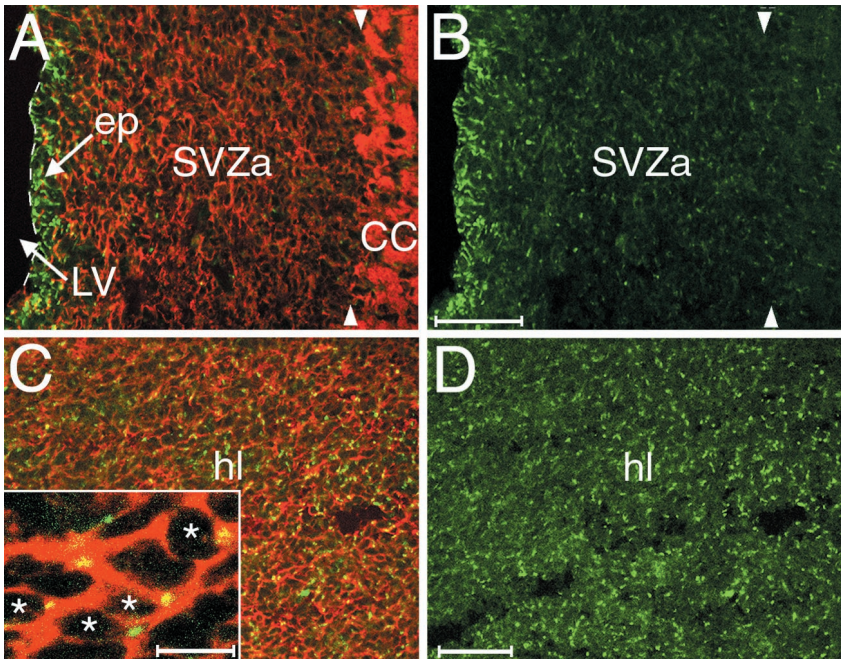

Figure 6. Expression pattern of p19^{INK4d} and neuron-specific tubulin by the cells of the neonatal rostral migratory stream. *A–D*, Representative confocal photomicrographic images of the P0 SVZa (*A, B*) and horizontal limb of the rostral migratory stream (RMS) (*C, D*) stained with an antibody to p19^{INK4d} (recognized by a fluorescein-conjugated secondary antibody) and with the neuron-specific antibody TuJ1 (recognized by a rhodamine-conjugated secondary antibody). *A* is the superimposition of the confocal images of the SVZa initially captured independently with the fluorescein (*B*) and rhodamine (data not shown) filters. The entire thickness of the SVZa, except for the ependymal cell layer, is stained with TuJ1. The ventricular lining is outlined by a *white dashed line*. Although the cells of SVZa (*A*) and the hl of the RMS (*C*) are TuJ1-immunoreactive, only the hl of the RMS has prominent p19^{INK4d} labeling (compare *B, D*; also see Fig. 5). The *inset* in *C* shows that the neurons in the hl of the RMS are double-labeled with TuJ1 and anti-p19^{INK4d} (*asterisks*). The p19^{INK4d} labeling is localized to the cytoplasmic–nuclear border, and in most of the migrating SVZa-derived cells, it is concentrated in the half of the cell closest to the leading process. The regions of the cell that stained with TuJ1 and anti-p19^{INK4d} appear *yellow*. *Arrowheads* in *A* and *B* demarcate the boundary between the SVZa and the overlying corpus callosum. Dorsal is *up*, and anterior is to the *right*. *CC*, Corpus callosum; *ep*, ependymal cell layer; *hl*, horizontal limb of the RMS; *LV*, lateral ventricle; *SVZa*, anterior part of the neonatal subventricular zone. Scale bars: *A–D*, 50 μm; *C, inset*, 10 μm.

telencephalic VZ can be divided into a predominantly p19^{INK4d}(+) sublamina, in the apical half of the VZ (VZl), and a predominantly p19^{INK4d}(−) sublamina, in the basal half of the VZ (VZu). Despite previous studies that have analyzed the genesis of cells in the VZ (Brand and Rakic, 1979; Luskin and Shatz, 1985; Menezes and Luskin, 1994; Bittman et al., 1997; Kornack and Rakic, 1998), a strict sublamination was not evident previously. We further demonstrated that p19^{INK4d} is localized to the cytoplasmic–nuclear border in both the apical domain of dividing VZ cells and postmitotic neurons. Moreover, p19^{INK4d} undergoes a set of subcellular rearrangements and varies in its distribution around the nucleus as a function of the laminar position of a cell. In contrast to telencephalic VZ cells, SVZa-derived neuronal progenitor cells of RMS exhibit a different developmental sequence of p19^{INK4d} expression. Our data suggest that the SVZa-derived cells undergo multiple rounds of cell division by repetitively downregulating their p19^{INK4d} expression. In addition, there was an anterior^{high}–posterior^{low} gradient of p19^{INK4d} expression along the RMS. We showed that the p19^{INK4d} expression persists in the postmitotic neurons arising in both the VZ and SVZa. Taken together, our findings indicate that after the newly generated neurons of the developing cerebral cortex leave the cell cycle, they remain forever postmitotic, whereas SVZa-derived cells may successively downregulate their p19^{INK4d} expression and reenter the cell cycle before becoming permanently postmitotic neurons of the olfactory bulb.

The pattern of p19^{INK4d} immunoreactivity in the telencephalic ventricular zone reveals distinct p19^{INK4d}(+) and p19^{INK4d}(−) sublaminae

It has long been known that the neuroepithelium of the developing telencephalon has two zones of proliferating cells, the VZ and the later-arising SVZ. In this study, we provide evidence that the VZ has two distinct subdivisions. On the basis of the expression of p19^{INK4d}, one sublamina, situated in the apical part of the VZ adjacent to the ventricular lining (the VZl), has predominantly p19^{INK4d}(+) cells, and the other sublamina, in the basal or upper half of the VZ (the VZu), contains mostly p19^{INK4d}(−) cells. We also showed that the VZl becomes wider relative to the VZu as neurogenesis proceeds, in agreement with the fact that the pool of postmitotic neurons increases as the dividing cell population is depleted.

Although previous studies, using *in situ* hybridization, have analyzed the expression pattern of the CDKIs in the developing mouse brain (Zindy et al., 1997b), to better understand the spatiotemporal distribution of p19^{INK4d} in the developing forebrain, immunocytochemical analysis is also required. *In situ* hybridization studies showed that the p19^{INK4d} mRNA was expressed throughout all laminae of the developing neocortex. From this finding it was concluded that it is present in both proliferating and differentiating cell populations of the cerebral cortex. In contrast, our immunocytochemical results showed a differential expression pattern of p19^{INK4d} among the different

layers of the developing cerebral cortex. Specifically, VZu progenitors that are in the S phase of the cell cycle do not express p19^{INK4d}. However, many cells in the VZl do express p19^{INK4d}, and most likely these are immature neurons that have withdrawn recently from the cell cycle. Furthermore, reports that regulation of CDKIs occurs at the post-translational level (Pagano et al., 1995) underscore the need for immunocytochemical analyses of their expression. Although our data demonstrate that p19^{INK4d} appears to be differentially regulated by the cells of the VZl and VZu, these data do not exclude the possibility that VZl progenitor cells temporarily express p19^{INK4d} before they initiate a new round of interkinetic nuclear migration.

A few studies have suggested that under specific circumstances, p19^{INK4d} is expressed by cells undergoing division, disputing the idea that p19^{INK4d} is only expressed by postmitotic cells. In particular, Hirai et al. (1995) and Thullberg et al. (2000) demonstrated the oscillation of p19^{INK4d} expression by cultured macrophages and fibroblasts, after they were induced to reenter the cell cycle from a quiescent serum-deprived state. In these cells, the p19^{INK4d} mRNA levels were low during G_1, highest in S, and low again as they approached the subsequent G_1. When retroviral-mediated gene transfer was used to express p19^{INK4d} constitutively in cultures of cycling fibroblasts, however, the cells were arrested at the G_1 phase. This indicates that in fibroblasts the induction of p19^{INK4d} during the G_1 phase is sufficient to block the G_1–S progression. Our data argue that the temporal sequence of expression of p19^{INK4d}, described for macrophages and fibroblasts, is not what occurs when the progenitor cells of the VZ undergo division *in vivo*. Instead, our analysis of the temporal pattern of p19^{INK4d} expression during interkinetic nuclear migration demonstrates that there is a negligible level of p19^{INK4d} expression when the VZ progenitor cells are in the S phase and indicates that p19^{INK4d} is expressed at high levels in the VZl by newly generated postmitotic neurons. An alternative explanation to the scenario that only postmitotic cells of the VZl express p19^{INK4d} is that some actively dividing VZ progenitor cells temporarily express p19^{INK4d} before they undergo another round of interkinetic nuclear migration. Although our studies cannot exclude this as a formal possibility for VZ cells, it is likely to be the case for the cells of the RMS. However, the cells situated within the SVZa show the highest levels of BrdU incorporation and the lowest levels of p19^{INK4d} expression. Therefore, we have proposed that cells traversing the RMS may undergo dedifferentiation before successive rounds of cell division. The different patterns of p19^{INK4d} expression exhibited by the dividing cells of the VZ and SVZa strengthen the conclusion that the kinetics of p19^{INK4d} expression during the cell cycle may be cell-type specific.

p19^{INK4d} expression in the neonatal rostral migratory stream is inversely correlated with the distribution of mitotically active cells

Previous studies have demonstrated that the SVZa has a higher proliferative capacity than the subependymal zone in the middle of the olfactory bulb (Menezes et al., 1995; Smith and Luskin, 1998). In agreement with the studies based on BrdU incorporation, our study demonstrated a spatiotemporal gradient of p19^{INK4d} expression by SVZa-derived cells all along the RMS; the cells of the subependymal zone expressed higher levels of p19^{INK4d} than did those of the proximal RMS. This anterior^{high}–posterior^{low} gradient indicates that the SVZa-derived cells withdraw from the cell cycle as they approach the olfactory bulb. In addition, the ependymal cells that line the lateral ventricles express significantly higher levels of p19^{INK4d} also in agreement with their low rate of BrdU incorporation and proliferation (Doetsch et al., 1999). Our data suggest that in contrast to VZ progenitor cells, the cell cycle kinetics of the SVZa-derived cells is differentially regulated by endogenous and/or exogenous signals, which permit their ongoing mitosis even though they express a neuronal phenotype.

The subcellular redistribution of p19^{INK4d} by postmitotic neurons as they undergo migration and differentiation

Our findings revealed systematic changes in the subcellular distribution of p19^{INK4d} as postmitotic neurons migrate from the VZ to the cortical plate, in addition to the differential expression of p19^{INK4d} by the cells in the sublaminae of the VZ (VZl vs VZu) (Figs. 2, 4). The changes that p19^{INK4d} undergoes are somewhat analogous to the differential subcellular distribution of proteins, such as Notch (Sestan et al., 1999), in the different layers of the developing cerebral cortex. Although the underlying mechanism(s) regulating the dynamic redistribution of p19^{INK4d} is not known, layer-specific regulatory signals could be involved.

Several studies have suggested that the phenotype of a cell is related to whether it is the product of a symmetric or asymmetric division. For example, during cortical development, the fate of a cell is believed to be established by the differential distribution of Notch to the postmitotic apical daughter cell and Numb to the proliferative basal daughter cell after an asymmetric cell division (Chenn and McConnell, 1995; Doe and Spana, 1995; Zhong et al., 1996). Although the specific functions subserved by p19^{INK4d} in the progenitor cells of the telencephalon have not been determined, our data suggest that when a VZ progenitor cell undergoes an asymmetric cell division, p19^{INK4d} becomes segregated to the cytoplasmic–nuclear border of the apical postmitotic daughter cell. The significance of the concentration of p19^{INK4d} in the SVZa-derived cells at the cytoplasmic–nuclear border, in the portion closest to the leading process, remains to be determined.

SVZa progenitor cells potentially dedifferentiate as they successively divide and migrate in the rostral migratory stream

Previous studies have demonstrated that the SVZa neuronal progenitor cells exhibit atypical properties of proliferation in comparison with other CNS progenitors. Specifically, SVZa progenitor cells continue to divide as they migrate despite expressing a neuronal phenotype. Our previous and current findings of the presence of numerous TuJ1(+)/BrdU(+) cells along the RMS substantiate the premise that SVZa-derived neurons are dividing and that large numbers of neurons are added to the rat olfactory bulb during postnatal life. Despite the presence of BrdU(+) cells in the RMS, we also demonstrated the expression of p19^{INK4d} all along the RMS. This raises a discrepancy because our analysis of the developing cerebral cortex has shown that p19^{INK4d} is expressed exclusively by postmitotic cells that no longer incorporate BrdU. Our results showing TuJ1(+)/p19^{INK4d}(−) neurons in the RMS in addition to BrdU(+)/p19^{INK4d}(+) cells may reconcile this apparent contradiction (Fig. 7). We propose that SVZa-derived cells in the RMS can downregulate their expression of p19^{INK4d} and undergo subsequent rounds of cell division and that they repetitively undergo dedifferentiation and division to generate the vast number of cells destined for the olfactory bulb.

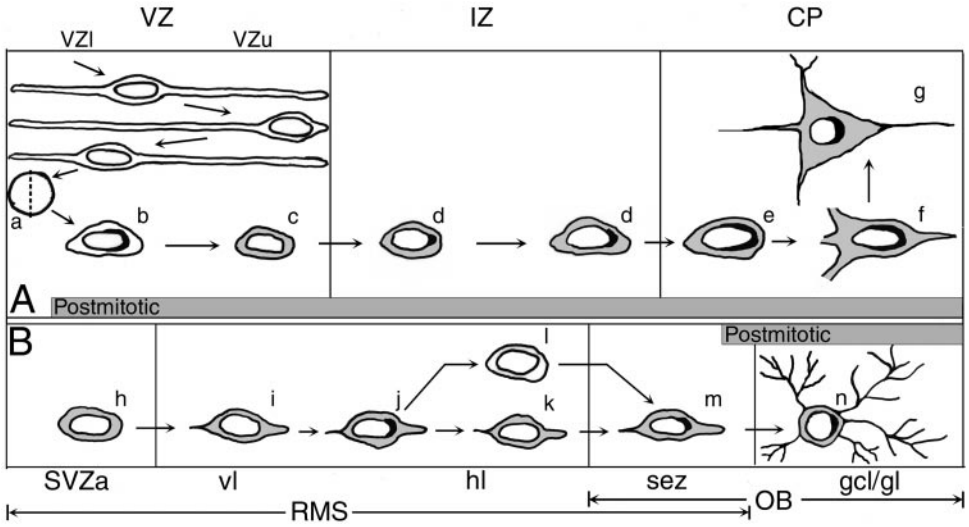

Figure 7. Summary of the subcellular rearrangements of p19^{INK4d} expression in the progeny of VZ cells compared with that of SVZa cells as they migrate from their site of origin to their destination. *A, B*, Diagrammatic representation of p19^{INK4d} localization in the cells of the developing cerebral cortex (*A*) and neonatal RMS (*B*) is shown. p19^{INK4d} expression is illustrated by *black shading* at the cytoplasmic–nuclear border, whereas cytoplasmic TuJ1 staining is illustrated by *gray shading*. The *horizontal bars* in *A* and *B* indicate the positions where postmitotic cells are present. *A*, The "life history" of a given progenitor cell and its progeny is diagramed in the *line drawing* of the developing cortex. After undergoing interkinetic nuclear migration, VZ progenitor cells of the embryonic telencephalon divide at the ventricular surface (*a*) and exit the cell cycle. Subsequently, postmitotic cells initiate differentiation and migrate to their final destinations in the cortical plate. While the progenitor cell is in the S phase of the cell cycle at the basal border of the VZ, it does not express p19^{INK4d}. However, when the progeny of the VZ progenitor withdraws from the cell cycle after undergoing asymmetrical (*a*) or symmetrical cell division in the VZl (data not shown), it exhibits substantial p19^{INK4d} expression (*b*). A migrating, immature postmitotic neuron (*c*) downregulates p19^{INK4d} expression as it passes through the VZu. Note that the immature neuron begins to be immunoreactive for the neuron-specific antibody TuJ1 in the VZu. After entering the intermediate zone, a migrating TuJ1(+) neuron (*d*) starts to express p19^{INK4d} in a punctate manner in its apical domain at the cytoplasmic–nuclear border. The p19^{INK4d} expression by cortical plate neurons (*e, f*) is more diffuse in comparison with that of the neurons of the intermediate zone (*d*). p19^{INK4d} expression persists in the differentiating postmitotic neurons of the cerebral cortex (*f*) represented by a pyramidal cell (*g*). *B*, The illustration demonstrates that the SVZa progenitor cells and their progeny are immunoreactive for the neuron-specific antibody TuJ1 at virtually all times, including at their site of generation the SVZa. However, there is negligible expression of p19^{INK4d} at this stage (*h*). While en route to the olfactory bulb, the SVZa-derived TuJ1(+) cells exhibit properties of migrating neurons including an elongated cell body and a leading process (*i–k*). In the proximal portion of the RMS, the SVZa-derived cell starts to express p19^{INK4d} at its apical pole (*j*). Because SVZa neuronal progenitors continue to divide as they migrate, we hypothesize that they may downregulate the expression of p19^{INK4d} (*k*) and reenter the cell cycle to undergo another round of cell division. Alternatively, they may downregulate both p19^{INK4d} and type III β-tubulin, indicating the possibility of dedifferentiation in the RMS (*l*). Although only one mitotic cycle is diagramed here, SVZa progenitors may undergo several rounds of cell division before reaching the subependymal zone in the middle of the olfactory bulb. In the olfactory bulb, the SVZa-derived cells show greater immunoreactivity for both TuJ1 and anti-p19^{INK4d} (*m*). The SVZa-derived cells terminally exit the cell cycle when they migrate into one of the overlying cellular layers of the olfactory bulb. The p19^{INK4d} persists in the postmitotic olfactory bulb interneurons within the gcl and gl (*n*). *CP*, Cortical plate; *gcl*, granule cell layer; *gl*, glomerular layer; *hl*, horizontal limb of the RMS; *IZ*, intermediate zone; *OB*, olfactory bulb; *RMS*, rostral migratory stream; *sez*, subependymal zone; *SVZa*, anterior part of the neonatal subventricular zone; *vl*, vertical limb of the RMS; *VZ*, ventricular zone; *VZl*, lower portion of the ventricular zone; *VZu*, upper portion of the ventricular zone.

REFERENCES

Bayer SA, Altman J, Russo RJ, Dai XF, Simmons JA (1991) Cell migration in the rat embryonic neocortex. J Comp Neurol 307:499–516.

Bittman K, Owens DF, Kriegstein AR, LoTurco JJ (1997) Cell coupling and uncoupling in the ventricular zone of developing neocortex. J Neurosci 17:7037–7044.

Brand S, Rakic P (1979) Genesis of the primate neostriatum: [3H]thymidine autoradiographic analysis of the time of neuron origin in the rhesus monkey. Neuroscience 4:767–778.

Casaccia-Bonnefil P, Hardy RJ, Teng KK, Levine JM, Koff A, Chao MV (1999) Loss of p27Kip1 function results in increased proliferative capacity of oligodendrocyte progenitors but unaltered timing of differentiation. Development 126:4027–4037.

Chenn A, McConnell SK (1995) Cleavage orientation and the asymmetric inheritance of Notch1 immunoreactivity in mammalian neurogenesis. Cell 82:631–641.

Doe CQ, Spana EP (1995) A collection of cortical crescents: asymmetric protein localization in CNS precursor cells. Neuron 15:991–995.

Doetsch F, Caille I, Lim DA, Garcia-Verdugo JM, Alvarez-Buylla A (1999) Subventricular zone astrocytes are neural stem cells in the adult mammalian brain. Cell 97:703–716.

Easter Jr SS, Ross LS, Frankfurter A (1993) Initial tract formation in the mouse brain. J Neurosci 13:285–299.

Edmondson JC, Hatten ME (1987) Glial-guided granule neuron migration in vitro: a high-resolution time-lapse video microscopic study. J Neurosci 7:1928–1934.

Hirai H, Roussel MF, Kato JY, Ashmun RA, Sherr CJ (1995) Novel INK4 proteins, p19 and p18, are specific inhibitors of the cyclin D-dependent kinases CDK4 and CDK6. Mol Cell Biol 15:2672–2681.

Kornack DR, Rakic P (1998) Changes in cell-cycle kinetics during the development and evolution of primate neocortex. Proc Natl Acad Sci USA 95:1242–1246.

Lee MK, Tuttle JB, Rebhun LI, Cleveland DW, Frankfurter A (1990) The expression and posttranslational modification of a neuron-specific beta-tubulin isotype during chick embryogenesis. Cell Motil Cytoskeleton 17:118–132.

Luskin MB (1993) Restricted proliferation and migration of postnatally generated neurons derived from the forebrain subventricular zone. Neuron 11:173–189.

Luskin MB, Boone MS (1994) Rate and pattern of migration of lineally-related olfactory bulb interneurons generated postnatally in the subventricular zone of the rat. Chem Senses 19:695–714.

Luskin MB, Shatz CJ (1985) Studies of the earliest generated cells of the cat's visual cortex: cogeneration of subplate and marginal zones. J Neurosci 5:1062–1075.

Menezes JR, Luskin MB (1994) Expression of neuron-specific tubulin defines a novel population in the proliferative layers of the developing telencephalon. J Neurosci 14:5399–5416.

Menezes JR, Smith CM, Nelson KC, Luskin MB (1995) The division of neuronal progenitor cells during migration in the neonatal mammalian forebrain. Mol Cell Neurosci 6:496–508.

Pagano M, Tam SW, Theodoras AM, Beer-Romero P, Del Sal G, Chau V, Yew PR, Draetta GF, Rolfe M (1995) Role of the ubiquitin-

proteasome pathway in regulating abundance of the cyclin-dependent kinase inhibitor p27. Science 269:682–685.
Raff MC, Durand B, Gao FB (1998) Cell number control and timing in animal development: the oligodendrocyte cell lineage. Int J Dev Biol 42:263–267.
Rakic P (1974) Neurons in rhesus monkey visual cortex: systematic relation between time of origin and eventual disposition. Science 183:425–427.
Sestan N, Artavanis-Tsakonas S, Rakic P (1999) Contact-dependent inhibition of cortical neurite growth mediated by notch signaling. Science 286:741–746.
Sherr CJ (1994) G_1 phase progression: cycling on cue. Cell 79:551–555.
Sherr CJ, Roberts JM (1999) CDK inhibitors: positive and negative regulators of G_1-phase progression. Genes Dev 13:1501–1512.
Smith CM, Luskin MB (1998) Cell cycle length of olfactory bulb neuronal progenitors in the rostral migratory stream. Dev Dyn 213:220–227.
Takahashi T, Nowakowski RS, Caviness Jr VS (1995) The cell cycle of the pseudostratified ventricular epithelium of the embryonic murine cerebral wall. J Neurosci 15:6046–6057.
Takahashi T, Nowakowski RS, Caviness Jr VS (1996) Interkinetic and migratory behavior of a cohort of neocortical neurons arising in the early embryonic murine cerebral wall. J Neurosci 16:5762–5776.
Thullberg M, Bartek J, Lukas J (2000) Ubiquitin/proteasome-mediated degradation of p19INK4d determines its periodic expression during the cell cycle. Oncogene 19:2870–2876.
Tikoo R, Osterhout DJ, Casaccia-Bonnefil P, Seth P, Koff A, Chao MV (1998) Ectopic expression of p27Kip1 in oligodendrocyte progenitor cells results in cell-cycle growth arrest. J Neurobiol 36:431–440.
Watanabe G, Pena P, Shambaugh III GE, Haines III GK, Pestell RG (1998) Regulation of cyclin dependent kinase inhibitor proteins during neonatal cerebella development. Brain Res Dev Brain Res 108:77–87.
Weinberg RA (1995) The retinoblastoma protein and cell cycle control. Cell 81:323–330.
Zhong W, Feder JN, Jiang MM, Jan LY, Jan YN (1996) Asymmetric localization of a mammalian numb homolog during mouse cortical neurogenesis. Neuron 17:43–53.
Zindy F, Quelle DE, Roussel MF, Sherr CJ (1997a) Expression of the p16INK4a tumor suppressor versus other INK4 family members during mouse development and aging. Oncogene 15:203–211.
Zindy F, Soares H, Herzog KH, Morgan J, Sherr CJ, Roussel MF (1997b) Expression of INK4 inhibitors of cyclin D-dependent kinases during mouse brain development. Cell Growth Differ 8:1139–1150.
Zindy F, Cunningham JJ, Sherr CJ, Jogal S, Smeyne RJ, Roussel MF (1999) Postnatal neuronal proliferation in mice lacking Ink4d and Kip1 inhibitors of cyclin-dependent kinases. Proc Natl Acad Sci USA 96: 13462–13467.